Department of Molecular Biology, Scripps Research Institute, La Jolla, California, 92037, USA.

7) $$$ 13135380 PMID: 8805536
Crystal structure of the yeast cell-cycle control protein, p13suc1, in a strand-exchanged dimer.
Khazanovich N; Bateman K; Chernaia M; Michalak M; James M
Medical Research Council Group in Protein Structure and Function, University of Alberta, Edmonton, Alberta, Canada T6G 2H7.

8) *** Crystal structure and mutational analysis of the Saccharomyces cerevisiae cell cycle regulatory protein Cks1: implications for domain swapping, anion binding and protein interactions.
Bourne Y; Watson M H; Arvai A S; Bernstein S L; Reed S I; Tainer J A
Centre National de la Recherche Scientifique, Marseille, France.
yves@afmb.cnrs-mrs.fr

Thank you.
MINH TAM DAVIS
ART UNIT 1642, ROOM 3A24, MB 3C18
272-0830

527071

10057, 813

1/31/05

16187579

Crystal structure and mutational analysis of the Saccharomyces cerevisiae cell cycle regulatory protein Cks1: implications for domain swapping, anion binding and protein interactions

Yves Bourne[1,2*†], Mark H Watson[2†], Andrew S Arvai[2], Susan L Bernstein[2], Steven I Reed[2] and John A Tainer[2]

Background: The *Saccharomyces cerevisiae* protein Cks1 (cyclin-dependent kinase subunit 1) is essential for cell-cycle progression. The biological function of Cks1 can be modulated by a switch between two distinct molecular assemblies: the single domain fold, which results from the closing of a β-hinge motif, and the intersubunit β-strand interchanged dimer, which arises from the opening of the β-hinge motif. The crystal structure of a cyclin-dependent kinase (Cdk) in complex with the human Cks homolog CksHs1 single-domain fold revealed the importance of conserved hydrophobic residues and charged residues within the β-hinge motif.

Results: The 3.0 Å resolution Cks1 structure reveals the strict structural conservation of the Cks α/β-core fold and the β-hinge motif. The β hinge identified in the Cks1 structure includes a novel pivot and exposes a cluster of conserved tyrosine residues that are involved in Cdk binding but are sequestered in the β-interchanged Cks homolog suc1 dimer structure. This Cks1 structure confirms the conservation of the Cks anion-binding site, which interacts with sidechain residues from the C-terminal α helix of another subunit in the crystal.

Conclusions: The Cks1 structure exemplifies the conservation of the β-interchanged dimer and the anion-binding site in evolutionarily distant yeast and human Cks homologs. Mutational analyses including *in vivo* rescue of *CKS1* disruption support the dual functional roles of the β-hinge residue Glu94, which participates in Cdk binding, and of the anion-binding pocket that is located 22 Å away and on an opposite face to Glu94. The Cks1 structure suggests a biological role for the β-interchanged dimer and the anion-binding site in targeting Cdks to specific phosphoproteins during cell-cycle progression.

Introduction

Cell-cycle regulation in the budding yeast *Saccharomyces cerevisiae* requires highly regulated transitions that are driven by activation of the Cdc28 cyclin-dependent kinase (Cdk) [1–6]. Genetic analyses have identified a number of proteins that interact with the Cdc28 kinase, including Cks1, which was isolated as a high-copy suppressor of a temperature-sensitive cdc28 mutation and designated Cdc28 kinase subunit (Cks) as a result of its association with cyclin–Cdc28 kinase complexes *in vivo* [7,8]. Although Cks1 is essential for cell-cycle progression *in vivo* and interacts genetically and physically with Cdc28 [7], its precise biological function has remained a mystery. Recent studies showed that suc1, the *Schizosaccharomyces pombe* Cks1 homolog interacts with an active form of the cyclosome [9], that Xe-p9, a *Xenopus* homolog of Cks1, interacts with Cdc27, a component of the cyclosome [10], and that Cks1 interacts with the yeast 26S proteasome [11]. We previously identified the structural determinants responsible for Cdk2–CksHs1 interaction from the solution of the crystal structure of the complex

[12,13], and used that information to explore the biological function of Cks1 using mutational analyses. Cks1 is the only protein in this family that contains an unusual stretch of 16 consecutive glutamine residues at the C-terminal end (Figure 1) [7], which might mediate protein–protein interactions [14], as well as a cysteine residue at position 90 that precedes the conserved β-hinge region.

Here, we present the atomic structure of the β-interchanged dimeric form of Cks1 and use comparative analysis with the crystal structure of the β-interchanged dimeric form of suc1 [15] to identify a novel pivot point controlling the Cks1 fold, assembly, and conserved molecular surface accessible for Cdc28 kinase recognition. This dual mode of quaternary structure has only been observed in a few oligomeric proteins [16,17]. Comparison of this Cks1 β-interchanged dimeric structure with that of suc1 [15] and CksHs2 [18] reveals that β-strand swapping between domains is a conserved attribute in this essential cell-cycle protein and, as such, is likely to be functionally important for regulating

Figure 1
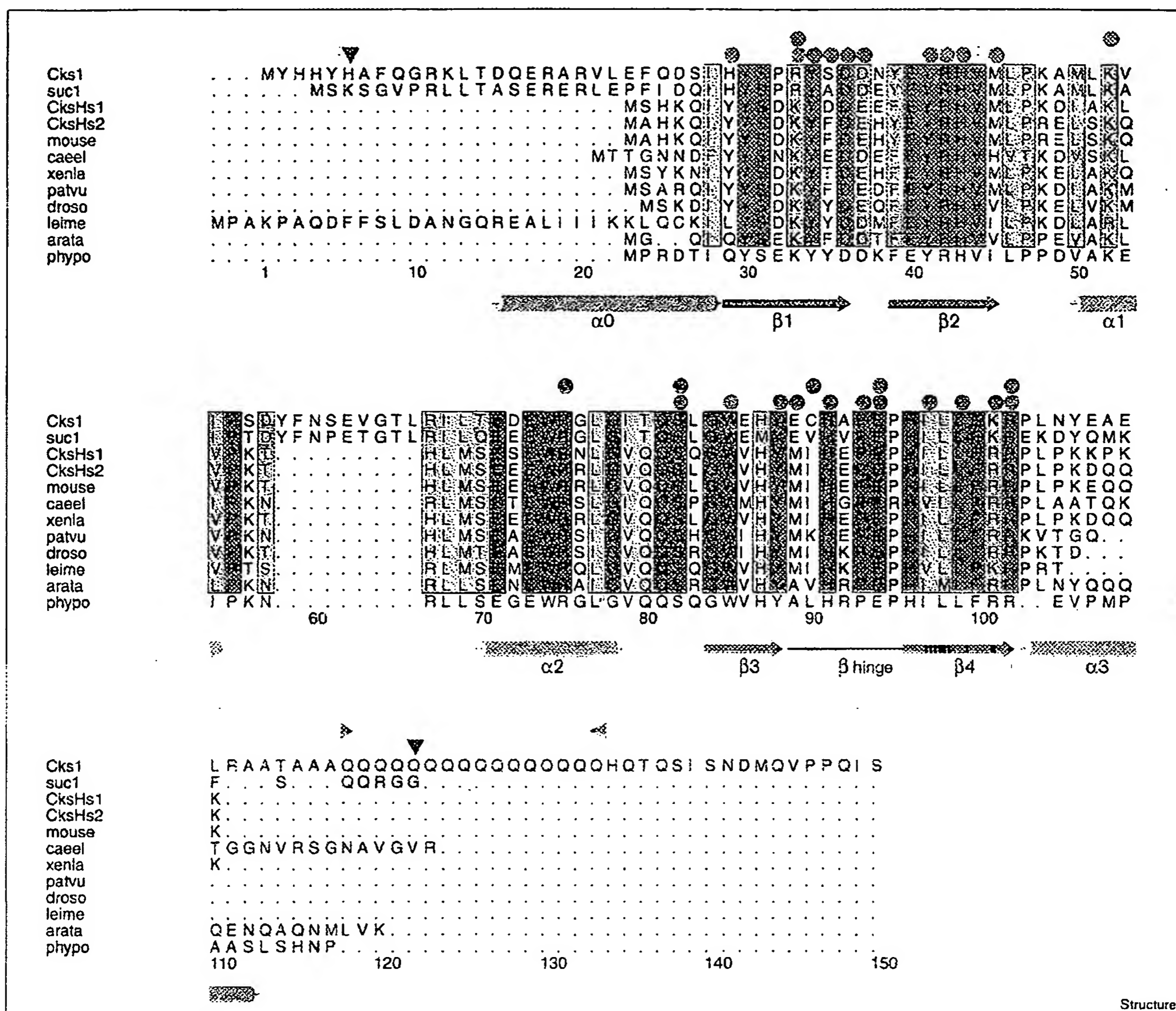
Sequence conservation, secondary structure, fold, assembly and residue function for Cks1 and homologous Cks proteins. The sequences of the two yeast homologs (Cks1 and suc1) are aligned with those of the two human (CksHs1 and CksHs2), mouse, *Caenorhabditis elegans* (caeel), *Xenopus* (xenla), *Patella vulgata* (patvu), fruit fly (droso), *Leishmania mexicana* (leime), *Arabidopsis thaliana* (arata) and *Physarum polycephalum* (phypo) proteins. The novel β-hinge region (Glu89–Cys90, dark blue bar) in Cks1 is marked together with the sequence-conserved region (His91–His96, red bar), which is conformationally similar in the β-interchanged suc1 dimer [15]. Residue functions inferred from the β-interchanged dimer Cks1 and other Cks structures are identified by symbols: mutated (red and blue circles for those that alter Cks1 function or maintain function, respectively) or deleted (left and right magenta arrows) residues, Cdk-binding site (green circles) and anion-binding site (orange circles). The position and identity of the four β strands and four α helices are also indicated: blue cylinders represent α helices and green arrows β strands. Black triangles mark the first and last residue present in the refined structure.

interactions with Cdks or other protein targets. Detailed comparison of this new Cks1 structure with the β-hairpin single-domain fold of suc1 [19], CksHs1 [20] and mutagenesis studies of CksHs2 [21], coupled with the present mutagenesis studies of Cks1, suggest regions in Cks proteins likely to be functionally important. The role of the β-hinge-motif conformation in regulating Cks1 binding to Cdks and that of the anion-binding pocket in targeting Cdks to other proteins or cellular structures are thought to be important.

Results

Structure determination and overall fold

The crystal structure of the *S. cerevisiae* protein Cks1 was determined by molecular replacement. Cks1 crystals are

hexagonal with space group P6₂22 (a = b = 106.5 Å and c = 166.5 Å), and contain three Cks1 molecules per asymmetric unit. The Cks1 structure was refined with noncrystallographic restraints against all diffraction data to an R factor of 21.6% and an R_{free} of 29.2% with good stereochemistry. The current Cks1 structure consists of three crystallographically independent subunits, each containing 106, 113 and 109 residues of the 150 possible residues, respectively, along with 16 solvent molecules. The structure is well defined overall, with only residues 4–7 at the N terminus and residues 25–29 at the C terminus being disordered. Despite the resolution limit of 3 Å, the excellent quality of the electron-density map unambiguously reveals the positions of the sidechains and carbonyl oxygens in the three Cks1 subunits (Figure 2a). Each Cks1 domain consists of a four-stranded β sheet and four flanking α helices (Figure 2b). These results indicate that, in addition to the conservation of the amino acid sequence and secondary structure, the overall canonical Cks1 fold is preserved among Cks proteins from human, fission yeast and budding yeast (Figure 1). Comparison with the structures of suc1 [15,19] reveals that Cks1 contains an additional C-terminal helix kinked towards the protein core at the non-conserved Pro103 position and a 16 glutamine residue tail (Figure 2b). Four of these glutamines are clearly visible in the electron-density maps.

The dominant and striking feature of the Cks1 subunit fold and dimer interaction is created by the C-terminal β strand, β4, which extends and exchanges with the identical strand from the other subunit in the dimer (Figure 2b). This β strand exchange, which requires an extended β-hinge-motif conformation, is dramatically different from those previously observed in the fission yeast suc1 [15] and human CksHs2 [18]. This difference is largely due to an additional pivot point immediately before the β-hinge motif. Furthermore, the Cks1 extended β hinge and β-strand exchange is stabilized by a disulfide bridge between the Cys90 residues from each subunit, which are absent in other Cks homologs. Despite these differences in the β-hinge region, the Cks1 core structure and hydrophobic packing are conserved in both yeast and human Cks structures, verifying the conserved fold and structure–function relationships (Figure 1). For example, the average root mean square deviation (rmsd) between Cks1 and suc1 domains is 0.69 Å for the mainchain atoms Gly10–Tyr88 and Glu94–Leu104, where Glu94–Leu104 belongs to the adjacent subunit, and 0.55 Å and 0.84 Å, respectively, for the mainchain atoms Ser27–Pro47, Ile68–His87 and Ile97–Leu104 of Cks1 and CksHs2 and of Cks1 and CksHs1.

The Cks1 protein can adopt either a β-hairpin single-domain fold or a β-interchanged dimeric structure, both of which are thermodynamically stable at physiological pH and ionic strength and can be purified separately from protein expressed in *Escherichia coli*. This multimerization

has also been observed for the fission yeast homolog suc1 [15,19]. Thus, distinct monomeric and dimeric structural forms of Cks proteins are conserved between distantly related *S. cerevisiae* and *S. pombe*. Human Cks proteins, CksHs1 and CksHs2, favor the Cks single-domain fold [20] and β-interchanged dimer [18], respectively. These results confirm that the swapped conformation exists for evolutionarily distant members of the Cks family of proteins, suggesting a functional role for β-strand swapping in cell-cycle control by Cks proteins.

Novel β-interchanged dimeric assembly

The presence of one and a half β-interchanged Cks1 dimers within the asymmetric unit and the existence of a β-interchanged dimer in fission yeast suc1 [15] and human CksHs2 [18] allows comparisons with both other Cks homolog structures and with the two non-equivalent β-interchanged Cks1 dimers. Superposition of the Cks1 and the suc1 β-interchanged dimeric structures reveals a strikingly different orientation of the sequence-conserved β-hinge motif HAPEPH (residues 91–96; single amino acid code) and the two subunits (Figure 3a). Although the overall conformation of this β-hinge motif is conserved between these two structures with an rmsd of 0.81 Å for all atoms and 0.54 Å for all backbone atoms (Figures 3b,c), this β-hinge region has moved as a rigid-body motion by over 10 Å in Cks1 in comparison with suc1, and this new position is well ordered in our crystal structure (Figure 2a). This Cks1 structure reveals a new pivot point located between residues Glu89 and Cys90 in Cks1, where a difference of 133° on ψ and 31° on φ for Cks1, compared with suc1, results in a dramatic change in the β-strand direction between the two β-interchanged dimeric structures. As a result, the second Cks1 subunit is rotated by approximately 180° relative to the first subunit when single subunits of Cks1 and suc1 are superimposed. Thus, Cks1 residues Val63–Thr65 in loop α1–α2 are roughly spatially equivalent to suc1 residues Asp33–Glu34 in loop β1–β2 (Figure 3a). Despite these surprisingly large orientational differences between the two subunit pairs, these two distinct β-interchanged dimeric structures each share overall dimensions of 45 × 35 × 25 Å and a total accessible surface area of 13,000 Å². In contrast, two distinct pivot points occur at positions Glu89 and Glu94 when the backbone conformation of the Cks1 and human CksHs2 β-interchanged dimer are compared, resulting in a different orientation of the second CksHs2 subunit. Superposition of the two crystallographically independent β-interchanged Cks1 dimers shows that each 'ECHA' region (residues 89–92) has a somewhat different conformation (Figure 3d). Considered independently, the structures of the core are virtually superimposable; however, the hinge-bending angle between the cores differs by 15° in a direction roughly perpendicular to the Cα–Cα vector of the residue pair His91–Ala92, verifying that this is a flexible hinge.

Figure 2
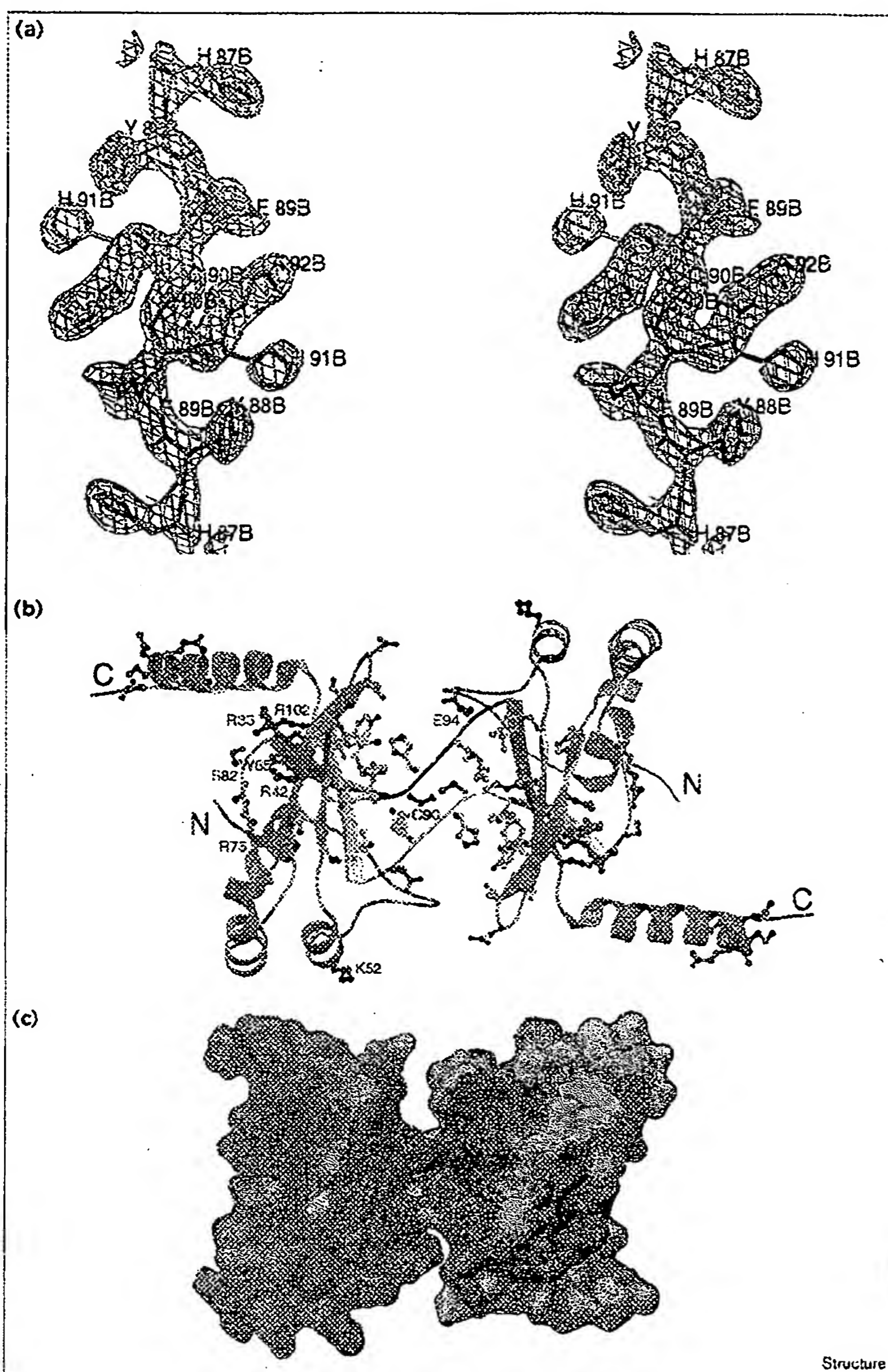
The Cks1 β-hinge region and overall fold of the β-interchanged Cks1 dimer. **(a)** Electron-density map and model for the Cks1 β-hinge region. Stereo pair of the 3 Å resolution F_o-F_c omit electron-density maps contoured at 2.0σ (black) and 4.0σ (magenta) around the two 87-HY ECHA-93 regions present in a Cks1 β-interchanged dimer. The coordinates of this region (5% of the total number of atoms) were omitted for each subunit and the protein coordinates refined by simulated annealing before the phase calculation. Residues are in yellow and blue for each subunit of the β-interchanged dimer. As verified by this electron-density map, the entire opened β-hinge region and the interdomain disulfide bridge are well ordered in the Cks1 crystal structure. **(b)** Ribbon model of the β-interchanged Cks1 dimer (yellow and blue subunits). The disulfide bridge between two adjacent Cys90 residues is displayed (orange bonds and yellow sulfur atoms). Four glutamine residues (ball-and-stick sidechains) are visible at the end of the C-terminal helical region, in which the last two adopt a β-strand conformation. Mutated sites (ball-and-stick sidechains) that destroy Cks1 function (red) and maintain function (green) as well as the anion-binding sidechains (polar atoms as red oxygen and blue nitrogen spheres) are shown. **(c)** The conserved and variable residue molecular surface to a 1.4 Å radius probe for the β-interchanged Cks1 dimer is oriented to match (b). Residue surface (red invariant, yellow highly conserved and blue nonconserved) is viewed looking down into the aromatic residue cluster within a sequence invariant surface residue patch (sidechains Tyr34, Tyr41, Tyr88, His91 and Glu94 of each subunit).

The major structural significance of the new β-hinge pivot point in Cks1 for Cdk binding is apparent from the complete exposure of the sequence-conserved tyrosine surface region (Figure 2c). The new β-interchanged Cks1 dimer dramatically alters the conserved-sequence accessible molecular surface when compared with suc1 or human CksHs2 dimers. A patch of sequence-conserved tyrosine residues (Tyr34, Tyr41 and Tyr88) along with His91 and Glu94 in both subunits are fully solvent accessible and are located on one face of the β-interchanged Cks1 dimer (Figure 2c). Although these same residues are also fully accessible for Cdk or other protein binding in the closed β-hairpin conformation of the β hinge in suc1 [19] and human CksHs1 [19], they are sequestered into a solvent-filled channel in both the β-interchanged suc1 dimer [15] and the hexameric assembly of human CksHs2

Figure 3

Cks1 fold and assembly compared with suc1. (a) The β-interchanged Cks1 dimer (yellow and blue subunits) superimposed with the suc1 dimer crystal structure (purple and green subunits) and shown as ribbons oriented to match Figure 2b. The black arrow indicates the pivot point in the residue pair Glu89–Cys90 for the conformational change observed between the β-interchanged Cks1 and the suc1 dimeric fold. Molecules superimposed according to the Cα atoms of residues Phe8–Glu89 for Cks1 (right, yellow subunit) and the equivalent suc1 residues (right, purple subunit). The adjacent Cks1 subunit (left) is rotated approximately 180° relative to that in suc1, resulting in the surprising substitutions of the Cks1 loop α1–α2 by the suc1 loop β1–β2 (top) and of the Cks1 loop β1–β2 by the suc1 loop α1–α2 (bottom). (b) The sequence conserved β-hinge region (His91–His96) in the β-interchanged Cks1 dimer (yellow tube) superimposed with the β-interchanged suc1 dimer (purple tube). This region shows a rigid-body motion in Cks1 compared with suc1 (bottom), with a new pivot point in the Cks1 residue pair Glu89–Cys90 (top). (c) Comparison of the sidechain orientations at the dimer interface between the β-interchanged Cks1 subunits (yellow and blue tubes) and the β-interchanged suc1 subunits (purple and green tubes). The superposition was carried out as in (a) but oriented 90° about the dimer twofold axis compared with (a). The reorientation of the His91 sidechain (suc1 His88) between the Cks1 and suc1 structures is shown (center), with suc1 His88 bound to the Asn57 and Glu59 sidechains (pink bonds and polar atom colored spheres, left), and Cks1 His91 bound to the Tyr85 sidechain (orange bonds and polar atom colored spheres, right). (d) Intrinsic flexibility of the β-hinge evident from the superposition of the two β-interchanged Cks1 dimers present in the asymmetric unit (subunits color-coded as the yellow–blue dimer and the purple–green dimers oriented to match Figure 2b). The locus of the bending region is His91–Ala92 (black arrow). Dimers were superimposed according to the Cα atoms of residues Phe8–Glu89. The yellow–blue dimer has the smallest hinge-bending angle.

[18]. However, the possibility of β-hinge opening and β-strand exchange blocking binding by bridging regions of the key recognition site [22] is not supported by the new Cks1 structure. As a result of the pivot between Glu89 and Cys90, no sequestering channel occurs for the Cks1 β-interchanged dimeric structure, leaving the conserved tyrosine region fully available for protein interactions. Although β-strand swapping is conserved in human, *S. pombe* and *S. cerevisiae* Cks1 homologs, the Cks1 dimer structure reveals that conserved Cdk interacting surface regions identified in the CksHs1–Cdk2 complex structure [12] are solvent exposed, suggesting that the functional role for β swapping might not be simply for sequestering conserved surface regions, but rather that it might modify the β-hinge region residue Glu94 in order to preclude Cdk binding.
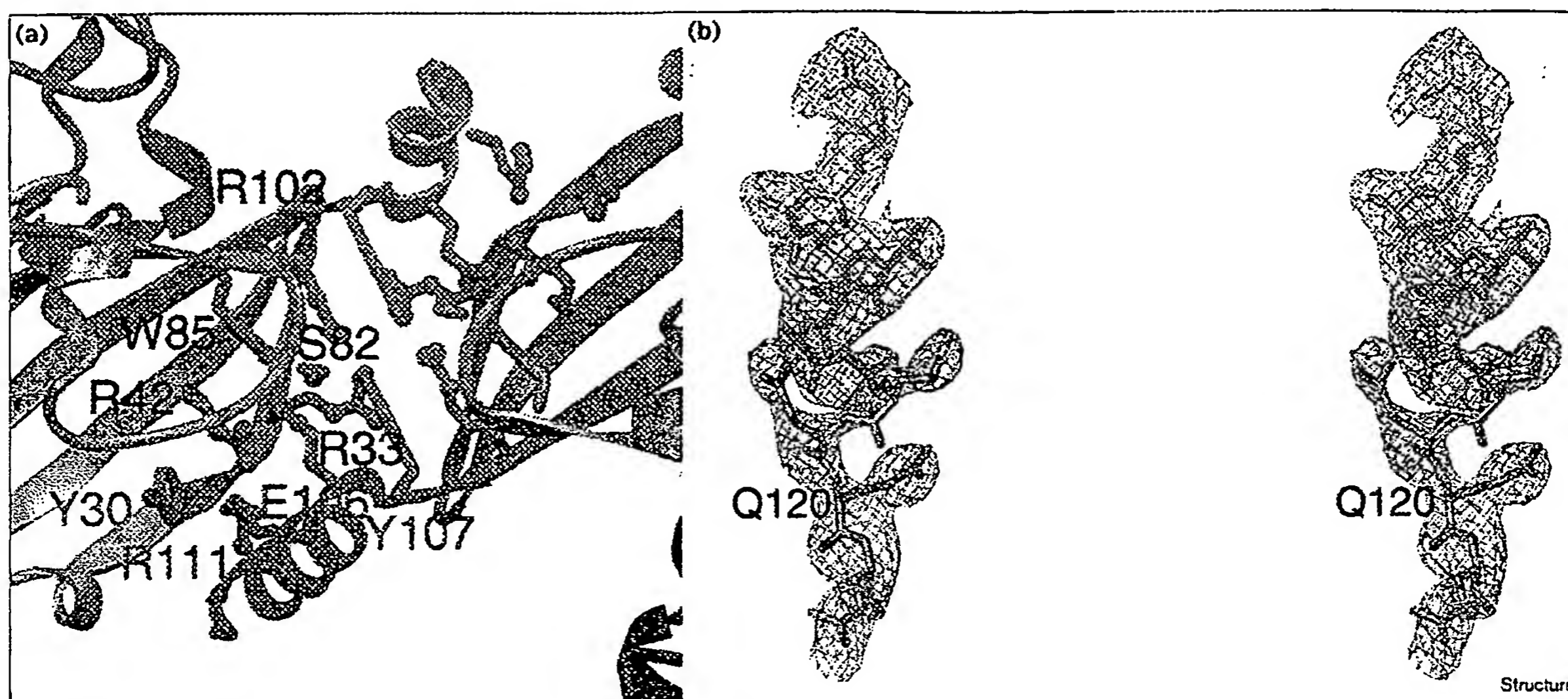
Anion-binding site

In addition to the new pivot point that dramatically alters the dimer's surface accessibility for Cdk interactions, the Cks1 structure reveals new interactions of the anion-binding site on a different Cks face. In each subunit a patch of conserved positively charged residues (Arg33, Arg42 and Arg102), along with Trp85 and Ser82, forms a sequence-conserved anion-binding site. The crystal structures of CksHs1 [19], CksHs2 [18] and suc1 [15] revealed anions
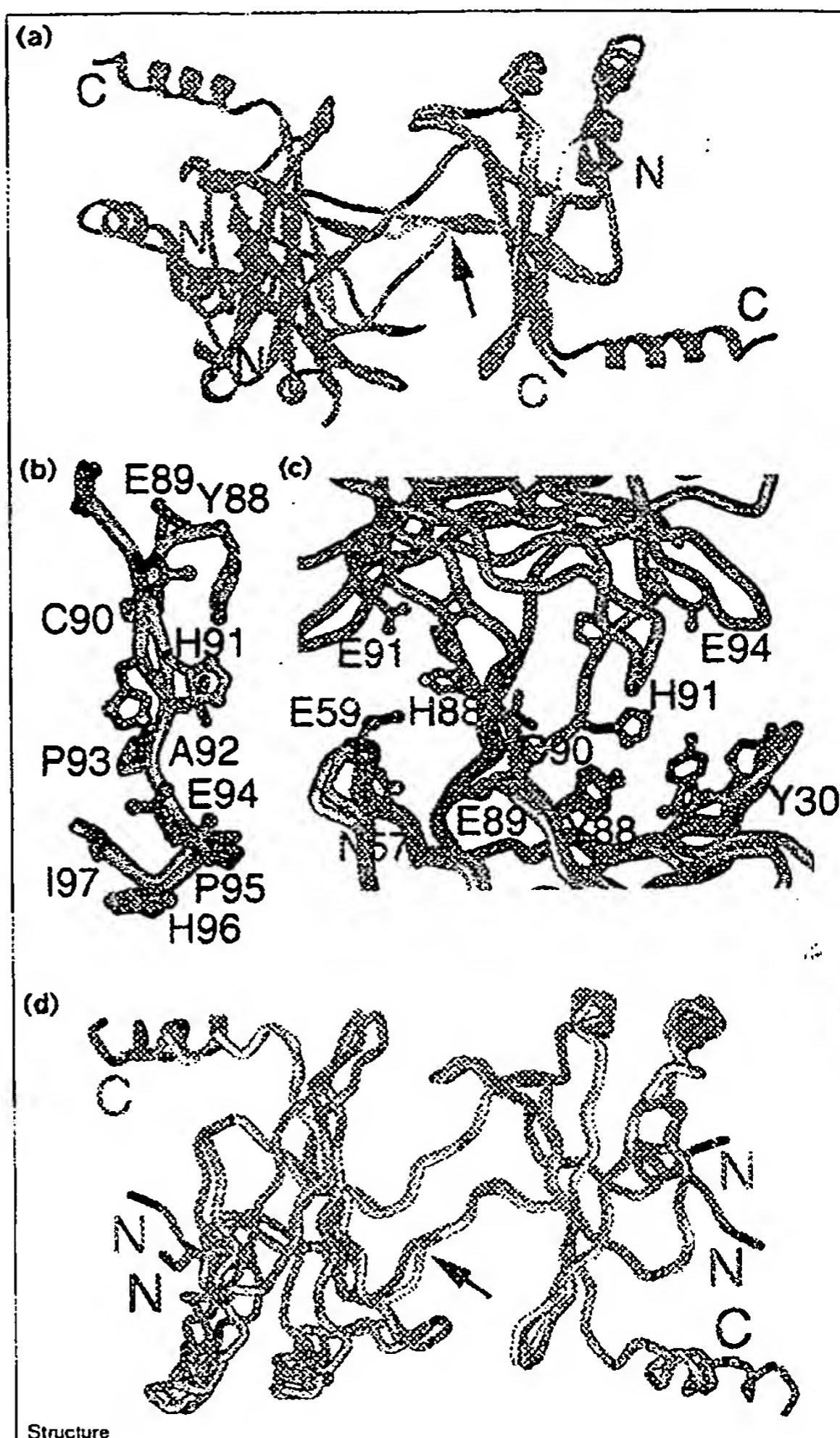
bound at this conserved pocket. There are no phosphate ions present in the Cks1 crystals because the anion-binding site is inaccessible to solvent as a result of the C-terminal α3 helix of an adjacent subunit in the crystal being bound at this site (Figure 4). This C-terminal α3 helix is unique to Cks1 (Figure 1). The corresponding region is unstructured in suc1, with the chain direction extended in a direction parallel to the last β4 strand across the crystal packing (Figure 3a). The presence of a nonconserved Pro103 in Cks1 bends the direction of this α3 helix, formed by residues Leu104–Ala112, along the protein surface. The α3 helix is further stabilized by van der Waals interactions between Leu83 and Leu110 sidechains. Helix α3 Tyr106 and Glu107 sidechains face the solvent and block the access of the anion-binding site in the adjacent subunit by establishing five hydrogen bonds: Tyr106–Arg102, Glu107–Arg42, Glu107–Trp85 and Glu107–Ser82 (Figure 4). In addition, the nonconserved β3 Arg111 interacts by stacking with Tyr30 of the adjacent subunit. Thus, the buried molecular surface area to a 1.6 Å radius probe of

Figure 4

Cks1 anion-binding site and glutamine tail. (a) Glu106 and Tyr107 residues (magenta bonds and polar atoms colored spheres) within the C-terminal helix α3 (not present in other Cks structures) bind to the five invariant residues (Arg33, Arg42, Arg102, Ser82 and Trp85, orange bonds) forming the anion-binding site located at the dimer interface of two β-interchanged Cks1 dimers (yellow and blue subunits). In addition, Arg111 in helix α3 stacks against Tyr30 in β1 (green bonds in this interdimer interface). (b) Electron-density map and model for the ordered position of the glutamine tail. Stereo pair of the 3 Å resolution $2F_o-F_c$ electron-density maps, contoured at 1.2σ, showing the first four glutamine residues, Gln118–Gln121, out of the 16 present in the Cks1 glutamine tail.

the β-interchanged Cks1 dimer in this tetramer conformation is 600 Å², which is slightly less than the β-hairpin single-domain suc1 dimer promoted by zinc (862 Å²) [19], but similar to the value of 650 Å² obtained at the tetramer interface of two β-interchanged suc1 dimers [15]. This Cks1 tetramer interface is particularly hydrophilic with a ratio of hydrophobic to hydrophilic surface area of 31:69 compared with a ratio of 65:35 found in most dimeric structures [23], suggesting that this interaction could be readily disrupted by interactions with phosphorylated proteins with high affinity for the anion-binding site.

Cks1 recognition processes

To test the biological role of Cks1 sequence-conserved surface regions in the β-hinge motif, the α helices, the anion-binding site and the polyglutamine tail for a possible recognition event, we constructed seven mutants of Cks1 (Table 1). First, we mutated the conserved Glu94 within the β-hinge motif to Gln (E94Q), to test the importance of this sidechain chemistry and negative charge. Second and third, we altered the anion-binding site by replacing a single positively charged Arg102 with Ala (R102A) and by combining three mutations (R33E, S82E, R102A). Fourth and fifth, we replaced conserved positively charged residues on each α helix, α1 residue Lys52 and α2 residue Arg75, by Glu (K52E and R75E) to test the functional importance of these two exposed charged residues on the protruding α-helical

structural elements. Sixth, we deleted the glutamine tail (Cks1-ΔGlntail) to test its biological importance in the *S. cerevisiae* Cks protein. Finally, we mutated Cys90 to Val, the analogous residue in the suc1 amino acid sequence, to evaluate the importance of the disulfide bridge for β-interchanged dimer formation and biological function.

The ability of these seven mutant *CKS1* alleles to function *in vivo* was tested in a yeast strain that has the chromosomal *CKS1* gene disrupted and is kept alive with a plasmid containing a wild-type copy of *CKS1* (see the Materials and methods section). Using this approach, the wild-type *CKS1* gene could be lost from cells that carried the plasmids with the wild-type *CKS1* and either *CKS1*-K52E or *CKS1*-R102A, *CKS1*-C90V or *CKS1*-ΔGlntail, but not from cells carrying either *CKS1*-R75E, *CKS1*-R33E/S82E/R102A or *CKS1*-E94Q. These results support the essential role of Cks1 and indicate that four mutant Cks1 proteins (K52E, R102A, C90V and ΔGlntail) retain their biological functions whereas the other three (α2 R75E, β-hinge E94Q and anion-binding pocket R33E/S82E/R102A) are non-functional (Table 1, Figure 2b). These mutagenesis results suggested a key role for the β hinge, the α2 helix and the anion-binding pocket in Cks function.

Next, we measured the ability of the wild-type and four Cks1 mutants (K52E, E94Q, R75E and R33E/S82E/R102A)

to bind to Cdc28 *in vivo* using the yeast two-hybrid system (Table 1). On the basis of this analysis, only the R75E and E94Q mutants were altered in their ability to interact with Cdc28, suggesting that the β-hinge region is an important Cks recognition site for Cdc28; this is consistent with the binding interface seen for the Cdk2–CksHs1 complex structure [12] and for the loss of interaction of the CksHs2 E63Q mutant with Cdk2 [21]. In contrast, the α2 R75E mutation, which is not located within the Cdk-binding interface, might have partially altered the Cks1 structure, thereby accounting for its inability to bind Cdc28 (see below). Taken together these Cks mutational analyses confirm the essential cell-cycle function of Cks proteins, identify the role of β-hinge binding of Cdc28 in Cks function, and suggest that α2 and/or the anion-binding pocket might function in binding a protein other than Cdc28.

Discussion

Monomeric and two distinct β-interchanged dimeric Cks structures in yeast

The β-interchanged Cks1 dimer is not stabilized by any loop–loop interactions such as those seen in suc1, with the ion or water-bridged interactions of negatively charged residues (suc1 Asp33–Glu35) from each subunit, but rather by the interdomain disulfide bridge. Modeling of a disulfide bridge in the β-interchanged suc1 dimer by replacing suc1 Val87 with its homolog Cys90 from Cks1 reveals a close van der Waals contact between suc1 Cys87 Sγ and the carbonyl oxygen atoms, suggesting that conformational change in the Cks1 residue pair Glu89–Cys90 was needed to favor a low-energy conformation of the disulfide bridge. The ability of Cks1 to form the β-hairpin single-domain fold seen for suc1 depends both on the β-hinge conformation and upon reduction of the interdomain disulfide formed by Cys90. However, this disulfide bridge might be strained, allowing reduction *in vivo*, as it presents an unusually large separation of the two Cα atoms (6.1–6.7 Å) resembling that in the immunoglobulin intrachain β strands [24]. Although intermolecular disulfide bonds are rare, they have been identified in proteins such as *S. cerevisiae* thioredoxin peroxidase [25] and transcription factor Pho4p [26], and they can be found in the swapped dimeric structure of bovine seminal RNaseA [27]. However, dimerization of bovine seminal RNAseA does not depend solely on the selective reduction of this intermolecular disulfide bridge [28], an observation that is in agreement with mutagenesis data of the Cks1 C90V mutant.

Interestingly, a detailed comparison of the β-hinge region between the β-hairpin single-domain fold suc1 and the β-interchanged suc1 dimer reveals a conformational difference located between suc1 Tyr85 and Glu86, in addition to the main difference between these two structures, which occurs within residues Val89 to Glu91 in the β-hinge region. Overall, the comparison of these two distinct Cks dimeric folds in yeast demonstrates a high flexibility within

Table 1

***In vivo* rescue of *CKS1* disruption and interactions of Cks1 probed by the β-galactosidase activities of Cdc28–Cks1 in the yeast two-hybrid assay.**

Cks1 protein	Structural location	Rescue of CKS1 disruption	β-Galactosidase activity (%)*
Wild type	–	+	100
K52E	α1 Helix	+	112 (± 5)
R75E	α2 Helix	–	29 (± 12)
C90V	Preceding β hinge	+	ND
E94Q	β Hinge	–	26.6 (± 9)
R102A	Anion-binding site	+	95 (± 23)
R33E, S82E, R102A	Anion-binding site	–	76 (± 9)
ΔGlntail(118–133)	PolyGln tail	+	ND

*The β-galactosidase activities are mean values of four independent experiments and are expressed as a percentage of the activity of wild-type constructs. ND, not determined.

the β-hinge region of this family of cell cycle regulatory proteins that could contribute to the regulation of the assembly of both the β-hairpin single-domain and the β-interchanged domain forms.

The new β-interchanged Cks1 dimer reveals an exposed aromatic cluster that is fully accessible for interaction both in the modeled monomeric and experimentally defined dimeric folds. If the β-interchanged dimerization regulates Cdk binding, then these results implicate the local β-hinge conformation directly in binding rather than indirectly by altering the accessibility of conserved aromatic residues. In the crystal structure of the human CksHs1–Cdk2 complex [12], CksHs1 binds Cdk2 in the single-domain fold with the bent β hinge and CksHs1 Glu63 (Cks1 Glu94) sidechain aligned with the direction of Cdk2 α5 helix and hydrogen bonded to two Cdk2 backbone nitrogen atoms. The Cks1 E94Q mutagenesis data are in agreement with those found for human CksHs1 [12] and human CksHs2 [21], which support a role for β-hinge conformational switching, rather than steric blocking, in regulating Cks1 binding to Cdc28.

Anion-binding site and protruding helical hairpin regions

The exposed conserved anion-binding site at the Cks1 molecular surface, consisting of residues Arg33, Arg42, Ser82, Trp85 and Arg102 and the protruding α2 helical hairpin region, might represent other recognition sites for either Cdks or other phosphorylated protein targets. Whereas removal of a single positive charge by mutation within the anion-binding site (R102A) does not alter Cks1 function or Cdc28 binding *in vivo*, a triple Cks1 mutant (R33E, S82E, R102A) abolishes the ability of the protein to rescue yeast lacking Cks1 but preserves Cdc28 binding.

These results suggest that the Cks anion-binding site might not be directed to Cdk2 Tyr160 as was previously proposed [18], but might instead be involved in binding to a Cdk substrate or to another phosphorylated target. Interestingly, Cks1 with mutation of the conserved but surface exposed Arg75 in helix α2 (R75E) close to the anion-binding site, which is not directly involved in Cdc28 binding, is also non functional *in vivo*, suggesting a biologically important recognition role for this Cks structural element that is distinct from Cdk binding. However, it is more likely that this mutation might cause some global disruption of the structure, which is not expected for protruding charged residues, or local conformational change at the molecular surface. In all known Cks structures the Arg75 sidechain is tightly anchored at the surface, and it establishes a van der Waals interaction with the Trp74 sidechain, and is hydrogen bonded to the Gln81 backbone oxygen atom located in surface loop α3–β3, and is salt bridged to the Glu71 sidechain located at the N-terminal cap of helix α3. In contrast, the equivalent CksHs1 Arg44 (Cks1 Arg75) sidechain is differently positioned in the CksHs1–Cdk2 complex and is not within hydrogen-bonding distance of CksHs1 Gln50 (Cks1 Gln81), allowing flexibility of the surface loop α3–β3. This suggests that the Arg75Glu mutation might destabilize the surface loop α3–β3 and indirectly affect Cdc28 binding. Further structural and biochemical experiments guided by these structural results will help to fully determine the biological role of the conserved surface-exposed α2 Arg75 residue.

For each of the three Cks1 subunits present in the asymmetric unit, the Glu107 residue in the C-terminal helix of one molecule binds to the anion-binding site of an adjacent molecule in the crystal. This resembles the packing of the suc1 Glu19 sidechain from the N-terminal α2 helix into the anion-binding site of the β-hairpin single-domain suc1 structure [19]. The helices are different in the two structures, however, and their direction is approximately perpendicular, suggesting that these crystal-packing contacts in Cks1 and suc1 might mimic the binding of a phosphorylated protein to the Cks1 anion-binding site. Both human CksHs1 and CksHs2 structures reveal bound cofactor anions such as vanadate, a phosphate analog [29], sulfate [18] and phosphate [21]. Similarly, the β-interchanged suc1 dimeric fold has a chloride ion tightly bound at the anion-binding site [15]. Whereas the aromatic cluster of residues is localized in the interior concave face of the β sheet and is important for Cdc28 binding [12], the anion-binding site and helical regions are positioned on the opposite side at the molecular surface, thus providing evidence for a possible dual recognition function of Cks proteins, a Cdk-binding site and a separate anion-binding site for a phosphoprotein, as demonstrated by the non-functional R75E mutation in both Cks1 and human CksHs2 (MHW and SIR, unpublished results) and the triple mutant (R33E, S82E, R102A) within the Cks1

anion-binding site. The fact that both suc1 and Xe-p9 bind to the phosphorylated active form of the cyclosome [9,10] and that Cks1 targets Cdc28 to the 26S proteasome during M-phase-specific proteolysis [11] suggests that these multiprotein complexes contain phosphorylated proteins that are recognized by the anion-binding pocket of Cks1. Identification of these anion binding pocket interacting proteins will contribute to understanding the mechanism by which Cks1 regulates progression of the cell cycle. Overall, these data support the bifunctionality of Cks proteins and suggest that Cks protein binding might be a mechanism for targeting Cdks during cell-cycle progression.

Glutamine tail

An unusual feature of the Cks1 amino acid sequence is the 16 consecutive glutamine residues at the C terminus. Although these glutamines are mostly disordered in our Cks1 crystal structure, four (residues 118–121) are visible in the electron-density maps of one Cks1 subunit. The last two glutamine residues clearly adopt an extended conformation that breaks the C-terminal α helix (Figure 4b). Glutamine repeats are known to form β conformations that might function as polar zippers, as is the case for specific transcription factors bound to separate DNA segments [13,30]. Our results using a Cks1 mutant deleted for the polyglutamine tail (Cks1-ΔGlntail) clearly indicate that it is not required for the biological function of Cks1 (Table 1). Therefore, the identification of the structural organization of the Cks1 glutamine tail will require the determination of new Cks1 crystal structures.

Conclusions

The comparison of the β-interchanged Cks1 dimer to other Cks structures identifies conserved and variable features of β-strand swapping that provides a structural basis for altering Cks1 functional interactions. The structural differences defined here between the β-interchanged dimer structures of Cks1 and those of suc1 and human CksHs2 indicate that these Cks regulatory proteins might adapt their conformation and assembly in response to environmental changes occurring at precise times during the cell cycle. Thus, these results suggest a potential novel structural mechanism for regulation of Cdk function based upon cooperative changes in Cks1 conformation and assembly. Biochemical and genetic characterizations of the mechanism that regulate the Cks monomer–dimer switch, aided by this Cks1 structural information, will be needed to establish the basis for regulation of Cdk function by Cks1. In addition, the identification of phosphoproteins that interact with the Cks1 anion-binding region, as characterized here, will also contribute to fully understanding the regulation of the cell cycle by the Cks proteins.

Biological implications

Cyclin-dependent kinase subunits (Cks) are small cell cycle regulatory proteins that share high sequence

identity from plants to humans and are essential for cell viability. Cks proteins lack catalytic function but are known to bind to cyclin–Cdk complexes during cell-cycle progression, and are thus an essential component of the cell-cycle machinery.

Domain swapping provides a mechanism by which cells can regulate the assembly of protein complexes by switching specific proteins between oligomeric states. The Cks1 structure reveals a novel β-interchanged dimer and establishes that the interchanged conformation exists for *Saccharomyces cerevisiae* as it does for the genetically distant *Schizosaccharomyces pombe*, supporting a functional role for β-strand swapping in cell-cycle control by Cks proteins. The mechanisms by which Cks proteins switch between monomeric and multimeric forms are not yet known; however, the results presented here, coupled with previous structural data, suggest that domain swapping within the family of Cks proteins might be involved in cell-cycle progression.

The structure-based mutagenesis data presented here, coupled with other recent genetic experiments, point to the novel dual functional role of Cks regulatory molecules that contain a Cdk-binding site with a sequence-conserved Glu94 within the β hinge and an anionic binding site located at the opposite face from Glu94 for an as yet unknown phosphoprotein, which could be a component of the yeast 26S proteasome.

Materials and methods

Site-directed mutagenesis
Specific amino acid changes were introduced into the *CKS1* gene, contained in the bacterial expression plasmid pRK171A [31], using the Transformer Mutagenesis Kit (Clontech Laboratories Inc. Palo Alto, CA) precisely as described by the manufacturer. The mutagenic primers were: R33E, 5'-GTGATAAGAGGCCTCATGAGTCTGCTA-3'; K52E, 5'-GGGATAACTTCTAGCATGGCC-3'; R75E, 5'-GATGCCGAGGC-CTTCCCATTCGTCTTC-3'; S82E, 5'-CCGTAGTGTGTCCTCAACC-CCACCCTT-3'; E94Q, 5'-ATGTGTGGTTGTGGCGCATGGC-3'; R102A, 5'-CGTAGTTCAGCGGCGCTTTGAATAGC-3'; ΔGlntail (118–133), 5'-CGATTGTGTTTGAT-GAGCAGCAGCGGTCGC-3'. The mutant *CKS1* sequences were amplified by the polymerase chain reaction (PCR) using flanking oligonucleotides containing *Bam*HI restriction sites and the products were cloned into the yeast galactose-inducible plasmid YCpG2 [32] and the two-hybrid *GAL4* transcriptional activation domain plasmid pACT2. The resulting constructs were confirmed by DNA sequencing and mutant Cks1 proteins were purified as described below for the wild type.

Yeast two-hybrid assays
CKS1 wild-type and mutant alleles (K52E, R75E, R33E/S82E/R102A, E94Q and R102A) were cloned into the *Bam*HI restriction site in the polylinker of the plasmid pACT2 to yield GAL4 transcriptional activation domain fusion constructs tagged with the haemaglutinin (HA) epitope and carrying the LEU2 marker. The CDC28 open reading frame was cloned into the *Bam*HI restriction site in the polylinker of the plasmid pAS1 [33] to produce a *GAL4* DNA-binding domain fusion construct tagged with the HA epitope and carrying the TRP1 marker. The pACT2 constructs were transformed into the haploid *S. cerevisiae* strain Y190 (*Mata gal4 gal80 his3 trp1-901 ade2-101 ura3- 52 leu2-3,-112+ URA3::GAL→lacZ, LYS2::GAL(UAS)→HIS3cyhr*) and selected on

plates lacking leucine. The pAS1-CDC28 construct was transformed into the haploid strain Y187 (*Mata gal4 gal80 his3 trp1-901 ade2-101 ura3-52 leu2-3.-112 met URA3:: GAL→lacZ*) and selected on plates lacking tryptophan. Yeast transformations were performed as described in [34]. Expression of the fusion proteins was confirmed by western blotting using a monoclonal antibody (12CA5) to the HA epitope. Quantitative matings and β-galactosidase assays were carried out as described in [21].

In vivo *rescue of* CKS1 *disruption*
The ability of the *CKS1* mutant alleles to function in vivo was determined as described in [21].

Crystallization and data collection
BL-21 *E. coli* containing the *CKS1* expression plasmid pRK171 was expressed and purified according to the protocol previously used for the *S. pombe* suc1 [15]. Crystals were obtained by the vapor-diffusion technique at 20°C after mixing the protein solution (12 mg/ml) with 20% PEG4K, 5% NaSCN (from a saturated solution) and 0.1 M imidazole/malate, pH 7.0. The crystals belong to the space group P6$_2$22 with cell dimensions a = 106 Å b = 106 Å and c = 166.5 Å, giving the Vm value of 2.5 Å^3/Da (51% solvent) for three Cks1 molecules in the asymmetric unit. A complete data set extending at 3 Å resolution, consisting of 243,609 observations for 10,366 unique reflections (91% complete, R$_{sym}$ = 9.4%), was collected from one crystal (0.15 × 0.15 × 50 μm) at beamline 7-1 of the Stanford Synchrotron Radiation Laboratory (SSRL) with a Mar-Research image plate. Crystals are highly sensitive to X-ray radiation and also do not diffract after being flash-cooled in the presence of various cryoprotectants. To overcome these problems, the crystal was mounted into a capillary, excess mother liquor removed, and then successfully flash-cooled at 100K. Oscillation images were integrated, scaled, and merged using DENZO [35] and SCALA [36].

Structure determination and refinement
Initial phases were obtained with molecular replacement using a truncated suc1 molecule (Protein Data Bank [PDB] code 1SCE [15]) as a search model with the AMoRe program package [37]. Residues Val6–Ser24 and the β-hinge region (residues His88–His93 together with Glu86 and Cys87) between β3 and β4 were removed from suc1 to achieve the correct orientation of our Cks1 model. The peak heights in the translation function of one truncated Cks1 molecule were used to solve the space-group ambiguity, and the corresponding phases were automatically used to screen all other rotation peaks. The model was refined using X-PLOR [38] and, in later stages, CNS version 0.5 [39]. After rigid-body refinement of the three molecules, the correlation and the R factor were 31.4% and 48%, respectively, in the 15 Å to 3.5 Å resolution range. Refinement using data between 8 Å and 3 Å gave an R factor of 34%. The β-hinge region and the preceding region were then built between two symmetry-related Cks1 molecules with the graphics program TURBO-FRODO [40] into both 2F$_o$-F$_c$ and F$_o$-F$_c$ electron-density maps, which clearly showed the presence of a disulfide bridge between two residues Cys90 belonging to adjacent subunits. Addition of the N and C termini and a conservative number of 16 solvent molecules resulted in a final R factor of 21.6% and an R$_{free}$ of 29.2% (5% of the reflections) for all 10,366 reflections in the 12 Å to 3 Å resolution range using noncrystallographic restraints. The final model comprises residues Phe8–Thr114, Phe8–Gln121 and Ala5–Thr114 for each of the three subunits, respectively, with overall deviations from ideal geometry of 0.015 Å for bond distances and 1.9° for bond angles. High temperature factors and weak electron density include residues Glu62–Gly64 in all three subunits. The rmsds are, respectively, 0.1 Å for tight noncrystallographic symmetry (NCS) restraint atoms, 0.19 Å for medium NCS-restraint atoms and 0.79 Å for lax NCS-restraint atoms between monomers A and B, and 0.1 Å, 0.32 Å and 1.1 Å between monomers A and C. The stereochemistry of the model was analyzed with PROCHECK [41] and WHAT-CHECK [42]; 84% of the polypeptide backbone dihedral angles were found to lie in the most-favored regions of the Ramachandran plot. Figure 1 was generated by Alscript [43], Figures 2a and 4b with TURBO-FRODO [40],

and Figure 2b with Molscript [44] and Raster3d [45], and Figures 2c, 3 and 4a with the Application Visualization System (AVS) (Advanced Visual Systems, Waltham, MA).

Accession numbers
The coordinates have been deposited in the PDB with accession code 1QB3.

Acknowledgements

References
1. Pines, J. & Hunter, T. (1991) Cyclin-dependent kinases: A new cell cycle motif? Trends Cell Biol. 1, 117-121.
2. Reed, S.I. (1992) The role of p34 kinases in the G1 to S-phase transition. Annu. Rev. Cell Biol. 8, 529-561.
3. Hunter, T. (1993) Braking the cycle. Cell 75, 839-841.
4. Dunphy, W.G. (1994) The decision to enter mitosis. Trends Cell Biol. 4, 202-207.
5. Morgan, D.O. (1995) Principles of CDK regulation. Nature 374, 131-133.
6. Morgan, D.O. (1996) The dynamics of cyclin dependent kinase structure. Curr. Opin. Cell. Biol. 8, 767-772.
7. Hadwiger, J.A., Wittenberg, C., Mendenhall, M.D. & Reed, S.I. (1989) The Saccharomyces cerevisiae CKS1 gene, a homolog of the Schizosaccharomyces pombe suc1+ gene, encodes a subunit of the Cdc28 protein kinase complex. Mol. Cell. Biol. 9, 2034-2041.
8. Tang, Y. & Reed, S.I. (1993) The Cdk-associated protein Cks1 functions both in G1 and G2 in Saccharomyces cerevisiae. Genes Dev. 7, 822-832.
9. Sudakin, V., Shteinberg, M., Ganoth, D., Hershko, J. & Hershko, A. (1997) Binding of activated cyclosome to p13(suc1). Use for affinity purification. J. Biol. Chem. 272, 18051-18059.
10. Patra, D. & Dunphy, W.G. (1998). Xe-p9, a Xenopus Suc1/Cks protein, is essential for the Cdc2-dependent phosphorylation of the anaphase-promoting complex at mitosis. Genes Dev. 12, 2549-2559.
11. Kaiser, P., et al., & Bailly, E. (1999) Cyclin-dependent kinase and Cks/Suc1 interact with the proteasome in yeast to control proteolysis of M-phase targets. Genes Dev. 13, 1190-1202.
12. Bourne, Y., et al. & Tainer, J.A. (1996) Crystal structure and mutational analysis of the human CDK2 kinase complex with cell cycle-regulatory protein CksHs1. Cell 84, 863-874.
13. Pines, J. (1996) Cell cycle: reaching for a role for the Cks proteins. Curr. Biol. 6, 1399-1402.
14. Perutz, M.F., Johnson, T., Suzuki, M. & Finch, J.T. (1994). Glutamine repeats as polar zippers: their possible role in inherited neurodegenerative diseases. Proc. Natl. Acad. Sci. USA 91, 5355-5358.
15. Bourne, Y., et al., & Tainer, J.A. (1995) Crystal structure of the cell cycle-regulatory protein suc1 reveals a β-hinge conformational switch. Proc. Natl. Acad. Sci. USA 92, 10232-10236.
16. Bennett, M.J., Schlunegger, M.P. & Eisenberg, D. (1995) 3D Domain swapping: a mechanism for oligomer assembly. Protein Sci. 4, 2455-2468.
17. Schlunegger, M.P., Bennett, M.J. & Eisenberg, D. (1997) Oligomer formation by 3D domain swapping: a model for protein assembly and misassembly. Adv. Protein Chem. 50, 61-122.
18. Parge, H.E., Arvai, A.S., Murtari, D.J., Reed, S.I. & Tainer, J.A. (1993) Human CksHs2 atomic structure: a role for its hexameric assembly in cell cycle control. Science 262, 387-395.
19. Endicott, J.A., et al., & Johnson, L.N. (1995) The crystal structure of p13suc1, a p34cdc2-interacting cell cycle control protein. EMBO J. 14, 1004-1014.
20. Arvai, A.S., Bourne, Y., Hickey, M.J. & Tainer, J.A. (1995) Crystal structure of the human cell cycle protein CksHs1: single domain fold with similarity to kinase N-lobe domain. J. Mol. Biol. 249, 835-842.
21. Watson, M.H., et al., & Reed, S.I. (1996) A mutation in the human cyclin-dependent kinase interacting protein, CksHs2, interferes with cyclin-dependent kinase binding and biological function, but preserves protein structure and assembly. J. Mol. Biol. 261, 646-657.
22. Endicott, J.A. & Nurse, P. (1995) The cell cycle and suc1: from structure to function? Structure 3, 321-325.
23. Janin, J., Miller, S. & Chothia, C. (1988). Surface, subunit interfaces and interior of oligomeric proteins. J. Mol. Biol. 204, 155-164.
24. Thornton, J.M. (1981) Disulfide bridges in globular proteins. J. Mol. Biol. 151, 261-287.
25. Jeong, J.S., Kwon, S.J., Kang, S.W., Rhee, S.G. & Kim, K. (1999) Purification and characterization of a second type thioredoxin peroxidase (type II TPx) from Saccharomyces cerevisiae. Biochemistry 38, 776-783.
26. Shao, D., Creasy, C.L. & Bergman, L.W. (1998) A cysteine residue in helix II of the bHLH domain is essential for homodimerization of the yeast transcription factor Pho4p. Nucleic Acids Res. 26, 710-714.
27. Mazzarella, L., Capasso, S., Demasi, D., DiLorenzo, G., Mattia, C.A. & Zagari, A. (1993). Bovine seminal ribonuclease: structure at 1.9 Å resolution. Acta Crystallogr. D 49, 389-402.
28. Piccoli, R., Tamburrini, M., Piccialli, G., DiDonato, A., Parente, A. & d'Alessio, G. (1992) The dual-mode quaternary structure of seminal RNase. Proc. Natl Acad. Sci. USA 89, 1870-1874.
29. Arvai, A.S., Bourne, Y., Williams, D., Reed, S.I. & Tainer, J.A. (1995) Crystallization and preliminary crystallographic study of human CksHs1: a cell cycle regulatory protein. Proteins 21, 70-73.
30. Gerber, H-P., et al., & Schaffner, W. (1994). Transcriptional activation modulated by homopolymeric glutamine and proline stretches. Science 263, 808-811.
31. Rosenberg, A.H., Lade, B.N., Chui, D.S., Lin, S.W., Dunn, J.J. & Studier, F.W. (1987) Vectors for selective expression of cloned DNAs by T7 RNA polymerase. Gene 56, 125-135.
32. Richardson, H.E., Stueland, C.S., Thomas, J., Russell, P. & Reed, S.I. (1990) Human cDNAs homologs of the small p34 cdc28/cdc2-associated protein of Saccharomyces cerevisiae and Schizosaccharomyces pombe. Genes Dev. 4, 1332-1334.
33. Durfee, T., et al., & Elledge, S.J. (1993) The retinoblastoma protein associates with the protein phosphatase type 1 catalytic subunit. Genes Dev. 7, 555-569.
34. Elble R. (1992) A simple and efficient procedure for transformation of yeasts. Biotechniques 13, 18-20.
35. Otwinowski, Z. & Minor, W. (1997) Processing of X-ray diffraction data collected in oscillation mode. Methods Enzymol. 276, 307-326.
36. Evans, P.R. (1997) Scala. Joint CCP4 and ESF-EACBM Newsletter. 33, 22-24.
37. Navazza, J. (1994) AMoRe: an automated package for molecular replacement. Acta Crystallogr. A 50, 157-163.
38. Brünger, A.T., Kuriyan, J. & Karplus, M. (1987) Crystallographic R-factor refinement by molecular dynamics. Science 235, 458-460.
39. Brünger, A.T., et al., & Warren, G.L. (1998) Crystallography & NMR system: a new software for macromolecular structure determination. Acta Crystallogr. D 54, 905-921.
40. Roussel, A. & Cambiliau, C. (1989) TURBO-FRODO. In Silicon Graphics Geometry Partners Directory (Silicon Graphics, ed.), pp. 77-78, Silicon Graphics, Mountain View, CA.
41. Laskowski, R.A., MacArthur, M.W., Moss D.S. & Thornton, J.M. (1993) PROCHECK: a program to check the stereochemical quality of protein structures. J. Appl. Crystallogr. 26, 283-291.
42. Hooft, R., Friend, G., Sander, C. & Abola, E. (1996). Errors in protein structures. Nature 381, 272.
43. Barton, G.J. (1993). Alscript: a tool to format multiple sequence alignments. Protein Eng. 6, 37-40.
44. Kraulis, P.J. (1991). Molscript: a program to produce both detailed and schematic plots of protein structures. J. Appl. Crystallogr. 24, 946-950.
45. Meritt, E. & Murphy, M. (1994). Raster3D version 2.0: a program for photorealistic molecular graphics. Acta. Crystallogr. D 50, 869-873.